Bull. Chem. Soc. Jpn., 72, 1465—1474 (1999)

Numerical Study on the Response of a Minimal Chemical Oscillator to an External Perturbation

Yoshihiro Sasaki

Institute for Chemical Research, Kyoto University, Uji, Kyoto 611-0011

(Received November 30, 1998)

The response of a sinusoidally perturbed minimal chemical oscillator was simulated over a wide range of perturbation parameters. Under a weakly perturbed condition, the system exhibited entrainment, quasiperiodicity and a Farey tree; under a more strongly perturbed condition, two types of chaos, small-amplitude oscillations and the coexistence of two oscillation modes were found. Phase-shifting of a kicked oscillator was considered in order to understand the entrainment.

Many chemical systems go back to thermodynamical equilibrium or steady states with exponential attenuation or damping oscillations when they are transiently perturbed. They also exhibit phase-shifting oscillations when they are perturbed periodically.[1,2] Relaxation phenomena, such as chemical relaxation in reaction systems and magnetic relaxation in spin systems, have been studied in regions near to thermodynamical equilibrium or steady points, where a linear response can be applied.[3] On the other hand, nonlinear reaction systems far from chemical equilibrium exhibit a variety of exotic behaviors (autonomous oscillations, multistability, etc.) based on their nonlinear properties.[4] The reaction systems existing in bistable states or in stable steady ones (foci) near to subcritical Hopf bifurcation points exhibit excitation against transient perturbations.[5,6] When periodic perturbations are added to autonomously oscillating nonlinear reaction systems, they respond to them in an interesting manner involving entrainment, quasiperiodicity and chaos, which are fundamental concepts concerning phenomena generated from interactions among nonlinear systems.[7,8] These concepts are also important in biological science.[9] Studies on forced chemical oscillators have been undertaken both experimentally and theoretically. A Brusselator has been used in numerical studies.[10,11] Homogeneous reaction systems, such as the Belousov–Zhabotinski (BZ) reaction[12,13] and a minimal oscillator,[14,15] electrochemical oscillators,[16] polymer gels,[17] and nervous systems[18—20] have been experimentally investigated. However, studies involving a minimal oscillator have been fragmentary. Computer simulations may be a good method to easily obtain a total image, compared with experiments. The behavior of a limit cycle stimulated by an external perturbation is presumably complicated. Thus, the author simulated the behavior of a forced minimal oscillator while attempting to sketch a global profile on the response of the oscillator to an external perturbation, and reports the result here. The Field–Körös–Noyes (FKN) mechanism used in this study is a realistic reaction mechanism, and the reduction of bromate by cerium(III) constitutes a part of the BZ reaction.[21] Taylor and Geisler undertook a similar investigation of a minimal oscillator.[14] Their report motivated the author to begin this study. However, our simulation was more detailed, and our results different from their's concerning some parts.

Calculations

The FKN mechanism described below reproduces the behavior of the bromate–bromide–cerium(III) reaction system in a continuous-flow stirred tank reactor (CSTR):[22—24]

$$Br^- + HBrO + H^+ \rightleftharpoons Br_2 + H_2O \quad (1)$$

$$Br^- + HBrO_2 + H^+ \rightarrow 2HBrO \quad (2)$$

$$Br^- + BrO_3^- + 2H^+ \rightleftharpoons HBrO + HBrO_2 \quad (3)$$

$$2HBrO_2 \rightarrow HBrO + BrO_3^- + H^+ \quad (4)$$

$$HBrO_2 + BrO_3^- + H^+ \rightleftharpoons 2BrO_2\cdot + H_2O \quad (5)$$

$$Ce^{3+} + BrO_2\cdot + H^+ \rightleftharpoons Ce^{4+} + HBrO_2 \quad (6)$$

In this calculation, we used the FKN mechanism and the FF set of rate constants prepared by Field and Försterling (Table 1).[25] Because the reaction system was assumed to be held in a CSTR, the $k_0(C_{0i} - C_i)$ terms were added to rate equations derived from Reactions 1—6, where C_i and C_{0i} are the concentrations of species i in the solution and in the feed flow, respectively, and k_0 is the reciprocal of the

Table 1. Rate Constants[a)]

Reaction	Forward	Backward
1	$8\times10^9\ M^{-2}\ s^{-1}$	$110\ s^{-1}$
2	$3\times10^6\ M^{-2}\ s^{-1}$	—
3	$2\ M^{-3}\ s^{-1}$	$3.2\ M^{-1}\ s^{-1}$
4	$3000\ M^{-1}\ s^{-1}$	—
5	$42\ M^{-2}\ s^{-1}$	$4.2\times10^7\ M^{-1}\ s^{-1}$
6	$8\times10^4\ M^{-2}\ s^{-1}$	$8900\ M^{-1}\ s^{-1}$

a) $1\ M = 1\ mol\ dm^{-3}$.

residence time. The external parameters for the system in a CSTR were $[BrO_3^-]_0$, $[Br^-]_0$, $[Ce^{3+}]_0$, $[H^+]_0$, k_0, and the temperature. The values of $[Br0_3^-]_0$, $[Br^-]_0$, $[Ce^{3+}]_0$, $[H^+]_0$, and the temperature were fixed, and k_0 was assumed to vary sinusoidally,

$$k_0 = \overline{k_0}(1 + \alpha \sin \omega_p t), \quad (7)$$

where $\overline{k_0}$ is the average of k_0. The values of $\overline{k_0}$ and the other external parameters used in this study are given in Table 2. Seven-variable equations were employed, since the $[H^+]_0$ value was very large.

Calculations of the steady states were performed by Newton's method. The stability of the steady states was analyzed by means of a linearized stability analysis. The temporal evolution of the system was calculated by using Gear's method.[26] The results, calculated up to 3×10^3 s, were ordinarily discarded in order to remove any influence of the initial values. The discarding time was 3×10^5 s at its maximum under the condition that a critical slowing down occurred. The calculated data were analyzed using a storoboscopic method and Fourier spectra. The bifurcation diagrams and return maps depicted in this study were prepared with numerical data on the Poincaré section ($\cos \omega_p t = 1$).

Results and Discussion

The reaction system existed in either of three states (SSI (a high concentration of Br^- and a low concentration of Ce(IV)), SSII (a low concentration of Br^- and a high concentration of Ce(IV)), and oscillations) under the conditions used in this study. Figure 1 shows the oscillatory region on the $k_0 - [BrO_3^-]_0$ plane, where the solid curves and the dashed one represent supercritical and subcritical Hopf bifurcations, respectively. The response of the minimal oscillator to the periodic perturbation given in Eq. 7 was simulated at points A and B. When the α value was large, the instantaneous steady point of the system migrated among the three states. It moved through supercritical Hopf bifurcations at point B and through both types of Hopf bifurcations at point A.

Simulation at Point A. Figure 2 shows typical oscillation patterns of $[Ce^{4+}]$, Poincaré sections ($\cos \omega_p t = 1$), return maps, and Fourier spectra of the oscillations under weakly perturbed conditions. In natural oscillations of the unperturbed system (a in Fig. 2), the period (T_0) and the frequency (ω_0) were 338 s and 0.0186 rad s^{-1}, respectively. If one wave of the oscillations of the entrained reaction system coincides with n (n: integer) waves of the k_0 oscillations, we say that the system is entrained in the $1/n$ harmonic mode. We can easily confirm that the state of the reaction system

Table 2. Reaction Conditions for CSTR

	Condition A	Condition B
$[H^+]_0$	0.75 M	
$[Ce^{3+}]_0$	3×10^{-4} M	
$[Br^-]_0$	2.9×10^{-4} M	
$[BrO_3^-]_0$	0.1 M	0.12 M
$\overline{k_0}$	0.005 s^{-1}	0.0064 s^{-1}

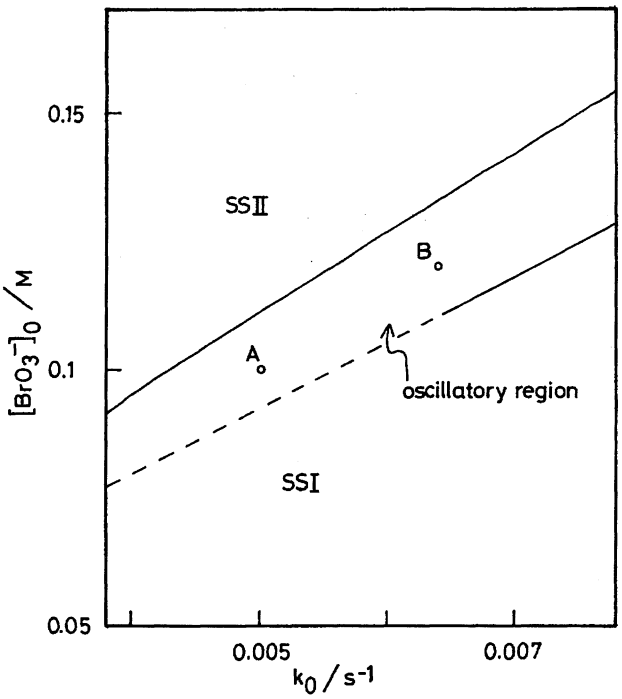

Fig. 1. Phase diagram of the minimal chemical oscillator in the k_0–$[BrO_3^-]_0$ parameter space.
$[H^+]_0 = 0.75$ M (1 M = 1 mol dm^{-3}), $[Ce^{3+}]_0 = 3\times10^{-4}$ M, and $[Br^-]_0 = 2.9\times10^{-4}$ M. Solid curves: supercritical Hopf bifurcation, dashed curve: subcritical Hopf bifurcation, and A and B: the points calculated in this study.

made a round during one wave of $[Ce^{4+}]$ oscillations when $\omega_p/\omega_0 \fallingdotseq 1$ (1/1 harmonic mode). Thus, we assume that the relation between the rotation of the state of the system and the oscillation pattern of $[Ce^{4+}]$ is conserved even in other harmonic modes, and we define the winding number (w) as follows, if the system is entrained in a $1/n$ harmonic mode and the number of peaks per one wave of $[Ce^{4+}]$ oscillations is given by m (m: integer):[27]

$$w = m/n. \quad (8)$$

When the ω_p value was 0.05 rad s^{-1}, we found a 1/3 harmonic mode and $w = 1/3$ (Fig. 2b), which were confirmed by the Poincaré section, the return map, and the Fourier spectrum of the $[Ce^{4+}]$ oscillations (Fig. 2b′, 2b″, and 2b‴, respectively). Figure 2c shows a quasiperidic state, which was characterized by the smooth Poincaré section, the smooth return map, and the noncommensurate peaks in the Fourier spectrum of the $[Ce^{4+}]$ oscillations (Fig. 2c′, 2c″, and 2c‴). We could thus recognize the "fundamental" harmonic mode, $1/n$ ($w = 1/n$), under the condition that $\omega_p/\omega_0 \fallingdotseq n$ when $\alpha = 0.05$. Figure 3 reveals another example that demonstrates the availability of the assignment of the harmonic modes. Figure 3a shows a bifurcation diagram between the fundamental 1/1 and the fundamental 1/2 entrainment bands, depending on the ω_p value. In the fundamental 1/2 entrainment, a period-doubling bifurcation occurred in front of its left side. Furthermore, "secondary" entrainment bands and quasiperiodic states were mutually found to exist between

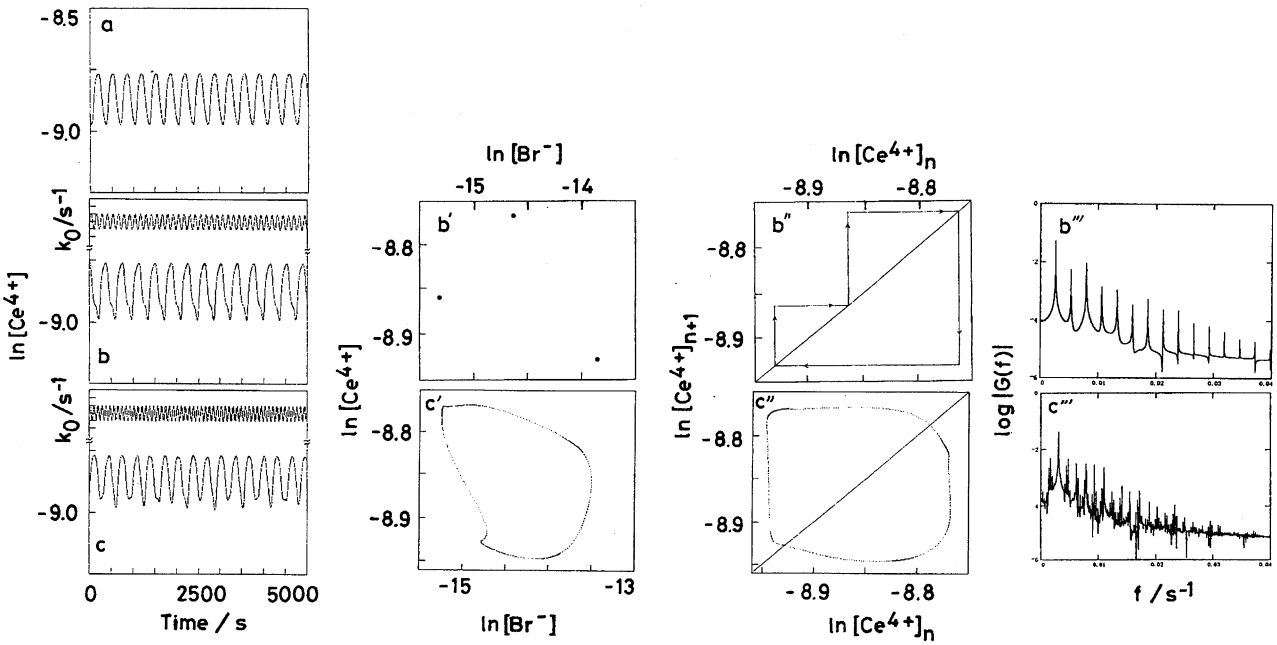

Fig. 2. Typical oscillation patterns of $[Ce^{4+}]$, Poincaré sections ($\cos \omega_p t = 1$), return maps, and Fourier spectra of the $[Ce^{4+}]$ oscillations.
The CSTR condition: A. $\alpha = 0.05$. a: natural oscillations ($\omega_0 = 0.0186$ rad s^{-1}). b (oscillation pattern), b′ (Poincaré section), b″ (return map), and b‴ (Fourier spectrum): $\omega_p = 0.05$ rad s^{-1} (1/3 (1/3) harmonic mode). c, c′, c″, and c‴: $\omega_p = 0.069$ rad s^{-1} (quasiperiodic mode). The fractions in the parentheses represent the assignment of the oscillatory mode entrained.

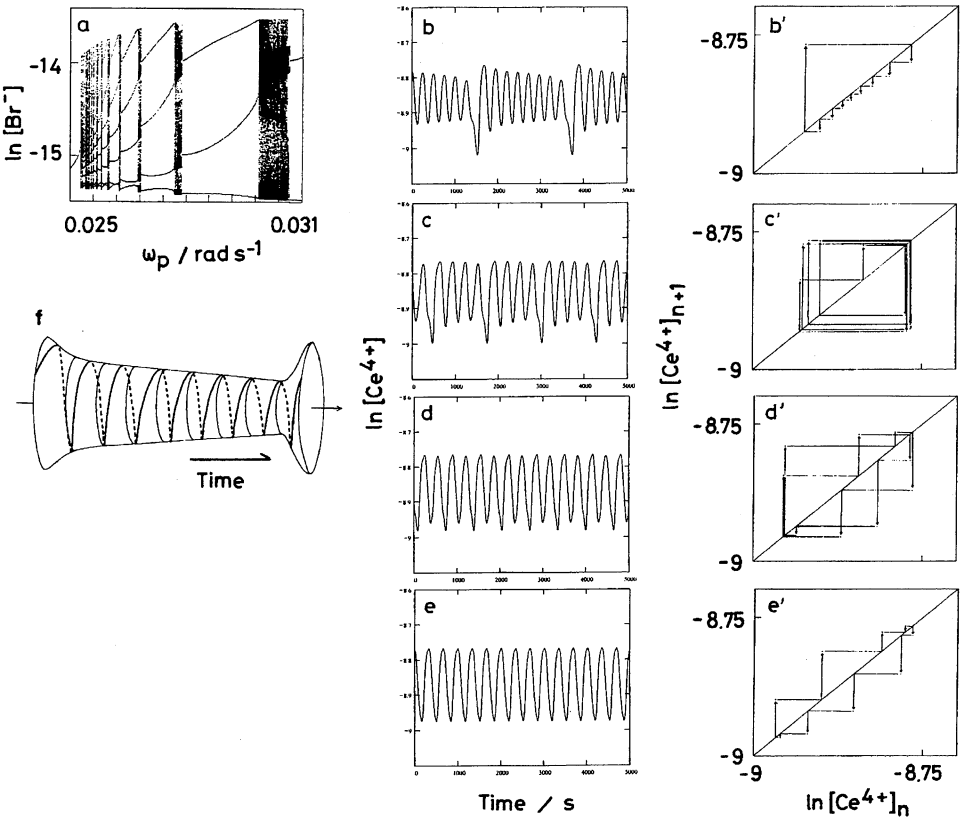

Fig. 3. Typical bifurcation diagram and assignment of oscillatory modes entrained.
The CSTR condition: A. $\alpha = 0.05$. a: bifurcation diagram between fundamental 1/1 and fundamental 1/2 entrainment bands, depending on the magnitude of ω_p. b (oscillation pattern of $[Ce^{4+}]$) and b′ (return map): $\omega_p = 0.02565$, and 1/9 (8/9) harmonic mode. c and c′: $\omega_p = 0.0445$, and 1/9 (4/9) harmonic mode. d and d′: $\omega_p = 0.0868$, and 1/9 (2/9) harmonic mode. e and e′: $\omega_p = 0.1684$, and 1/9 (1/9) harmonic mode. f: a supposed attractor of the 1/9 (8/9) harmonic mode in two components-time space. The unit of ω_p is rad s^{-1}.

the fundamental entrainment bands, where the secondary harmonic modes were assigned to $1/n$ ($(n-1)/n$) according to Eq. 8. For example, the harmonic mode under the condition that $\omega_p = 0.02565$ rad s^{-1} was assigned to 1/9 (8/9) (Fig. 3b). Other 1/9 harmonic modes, which appeared under the condition that $\alpha = 0.05$, were also assigned as follows: $w = 4/9$ when $\omega_p = 0.0445$ rad s^{-1} (Fig. 3c), $w = 2/9$ when $\omega_p = 0.0868$ rad s^{-1} (Fig. 3d), and $w = 1/9$ when $\omega_p = 0.1684$ rad s^{-1} (Fig. 3e). We also used another assignment based on return maps, in which points above and below the diagonal were allocated to symbols L and R, respectively. For example, the harmonic modes in Fig. 3b′ and 3c′ were written as LRRRRRRRR and LLRLRLRLR, respectively. The characteristics of Fig. 3c′, 3d′, and 3e′ (number of the points and rotation number) correspond to the winding numbers 4/9, 2/9, and 1/9, respectively. However, Fig. 3b′ is different in nature from the winding number, 8/9. We depict a supposed attractor of 1/9 (8/9) harmonic mode in two-component time-

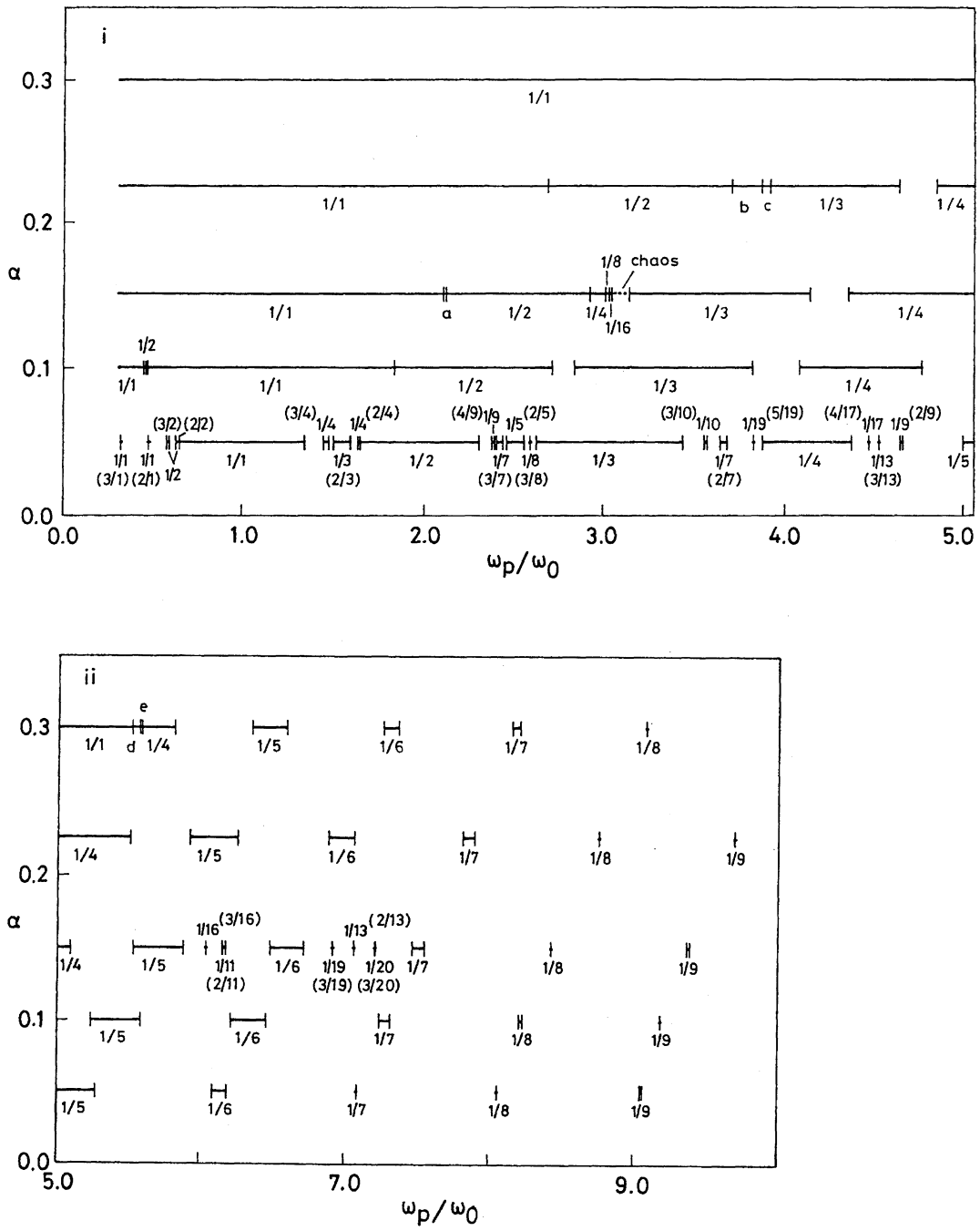

Fig. 4. Entrainment bands (I).

The CSTR condition: A. a: coexisting region of 1/1 and 1/2 harmonic modes, b: coexisting region of 1/2 and 1/3 harmonic modes, c: coexisting region of 1/1 and 1/3 harmonic modes, d: coexisting region of 1/1 and 1/4 harmonic modes, and e: coexisting region of 1/4 harmonic and quasiperiodic modes. The numbers in the parentheses represent winding numbers.

space in Fig. 3f (time interval: $\omega_p t = (2\pi)\times 9$), which gives visual images of the concepts, winding number, torus, and quasiperiodicity. Namely, the quasiperiodic mode in Fig. 3a corresponds to such oscillations whose attractor covers all over the surface of a torus. We can also suppose similar attractors for the other 1/9 harmonic modes. The methods used for the assignment were also used to classify all of harmonic modes observed in this study and in another one concerning chaos.[28] The assignment based on return maps was particularly effective in distinguishing two coexisting harmonic modes, as described in Ref. 28. The winding numbers obtained in this study constituted a Farey series, which suggests that the numbers are similar to the winding numbers used in a sine-circle map.[29]

The entrainment bands in the ω_p–α plane are shown in Fig. 4. The numbers in the parentheses represent winding numbers defined by Eq. 8. In the fundamental 1/1 and 1/2 entrainments, period-doubling bifurcations occurred in front of their left-hand sides. The width of the fundamental entrainment bands increased along with an increase in the α value in Eq. 7 (so-called Arnol'd tongues). Especially the 1/1 harmonic mode grew, and finally took down the 1/2 and 1/3 harmonic modes. Then, some new phenomena, such as chaos, small-amplitude oscillations and the coexistence of two oscillation modes, occurred. Figure 5 shows bifurcation diagrams between the fundamental 1/2 and fundamental 1/4 entrainment bands under the condition that $\alpha = 0.15$. As the ω_p value increased, the reaction system existing in the 1/2 harmonic mode changed to exhibit successive period-doubling bifurcations, and reached a chaotic mode (Feingenbaum ratio: 4.7). With a further increase in the ω_p value, the system changed from the chaotic mode to the 1/3 harmonic mode via an intermittency route.[30] Between the 1/3 and 1/4 entrainment bands, quasiperiodic states and period-doubling bifurcations (and perhaps chaotic states) were observed, and the bifurcation structure in this region was very complicated. Figure 6 shows a typical chaotic behavior ($\alpha = 0.15$ and $\omega_p = 0.058$ rad s^{-1}). A band constituted by Fourier components was observed in the Fourier spectrum (Fig. 6b) of the $[Ce^{4+}]$ oscillations (Fig. 6a), suggesting chaotic oscillations of this system. The Fourier component observed at about 0.0092 s^{-1} and its higher harmonics indicate that the system is driven by a periodic perturbation having a frequency of 0.058 rad s^{-1}. The Poincaré section ($\cos \omega_p t = 1$) in Fig. 6c was not ring-shaped. The shape suggests that the torus would collapse under this condition, and that the system exists in a chaotic mode. On the other hand, a Farey tree appeared between the fundamental 1/5 and 1/7 entrainment bands under the condition that $\alpha = 0.15$; we can probably also observe it between other entrainment bands. When the α value increased by more than 0.15, small-amplitude oscillations and the coexistence of two oscillation modes appeared. Figures 7a and 7b show the coexistence of the 1/3 and 1/2 harmonic modes, where the state of the reaction system was dependent on the initial values ($\alpha = 0.225$ and $\omega_p = 0.0705$ rad s^{-1}).[30] The oscillations of $[Ce^{4+}]$ in Fig. 7b are typical small-amplitude oscillations. The attractors of these harmonic oscillations are shown in the ($[Ce^{4+}]$, $[Br^-]$, $[BrO_2\cdot]$) subspace (1/3 modes: single loop (with a kink or a knot) (Fig. 7a′) and 1/2 harmonic mode: double loops (Fig. 7b′)). The attractor of the 1/2 harmonic mode was assigned to 1/2 ($w = 2/2$), suggesting that the harmonic mode was generated by a period-doubling bifurcation of a 1/1 harmonic mode (of small amplitude (Fig. 4)). The return maps of the $BrO_2\cdot$ species is shown in Figs. 7a″ and 7b″. The characteristics of these figures were a relatively large range of the 1/3 harmonic mode and a relatively small range of the 1/2 harmonic mode. The characteristics in return maps was successively observed in the coexistence of a 1/3 harmonic mode and a chaotic mode (α: ca. 0.18).[28] Figure 8 shows the coexistence of a 1/4 harmonic mode and a quasiperiodic mode. The quasiperiodicity appearing in Fig. 8a was supported by the Poincaré section and the return map (Figs. 8c and 8d, respectively). In this case, the quasiperiodic attractor exhibited small amplitudes. The quasiperiodicity seems to be different in nature from the quasiperiodicity estimated under the condition that $\alpha = 0.05$, because a torus is not defined in the case of two coexisting

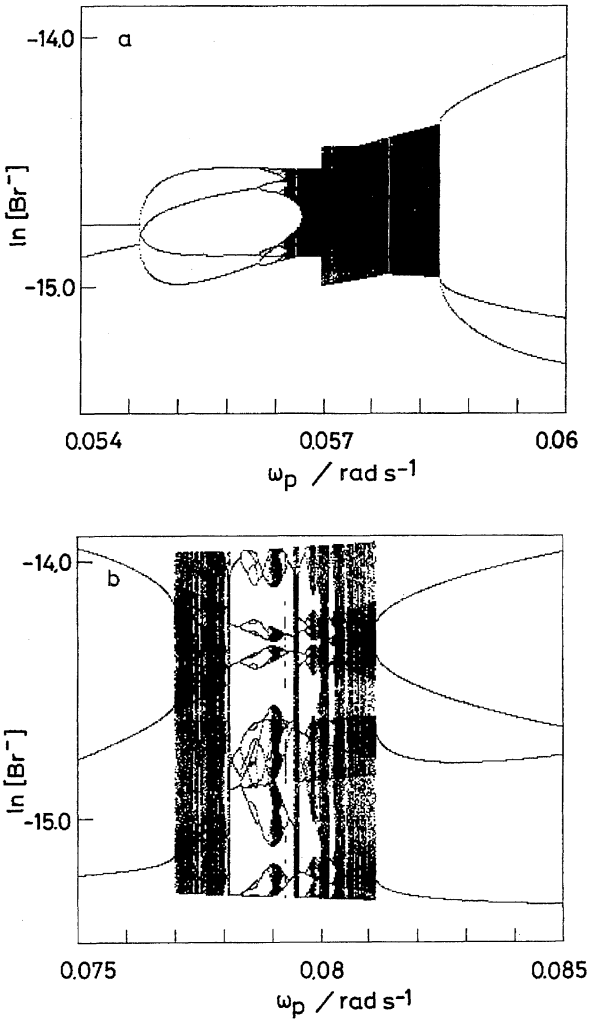

Fig. 5. Bifurcation diagrams depending on the magnitude of ω_p. $\alpha = 0.15$. a: between fundamental 1/2 and fundamental 1/3 entrainment bands, and b: between fundamental 1/3 and fundamental 1/4 entrainment bands.

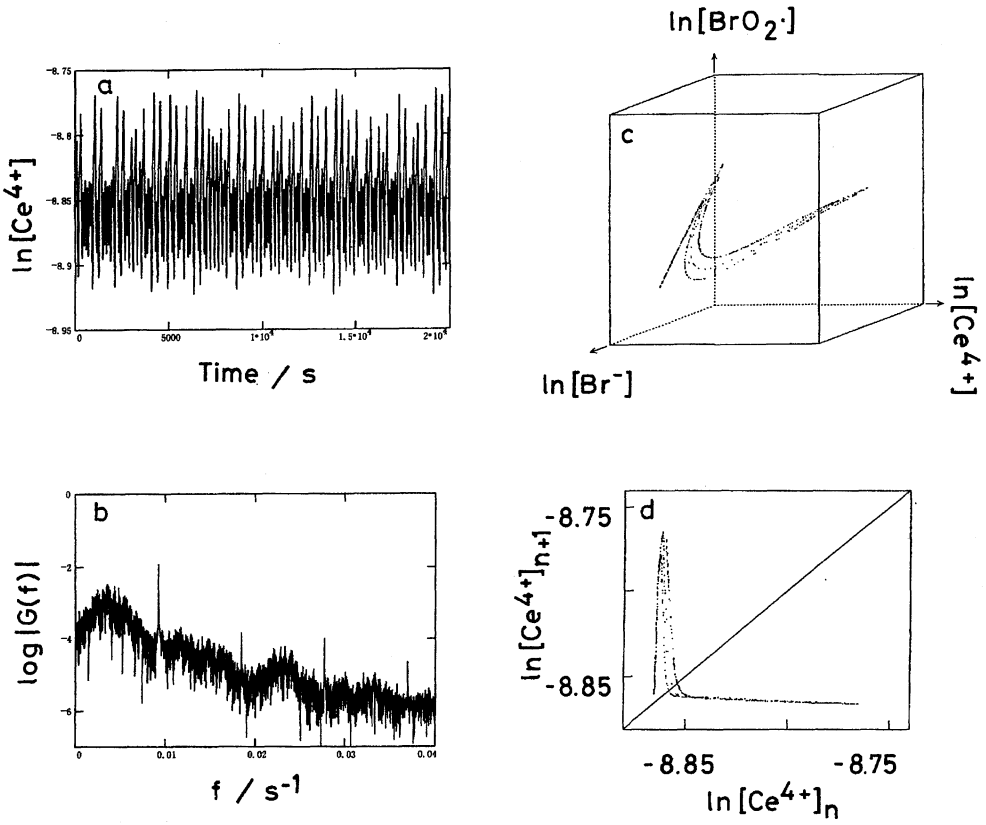

Fig. 6. Chaotic mode (I). $\alpha = 0.15$ and $\omega_p = 0.058$ rad s^{-1}. a: oscillation pattern of [Ce^{4+}], b: Fourier spectrum, c: Poincaré section (cos $\omega_p t = 1$), and d: return map.

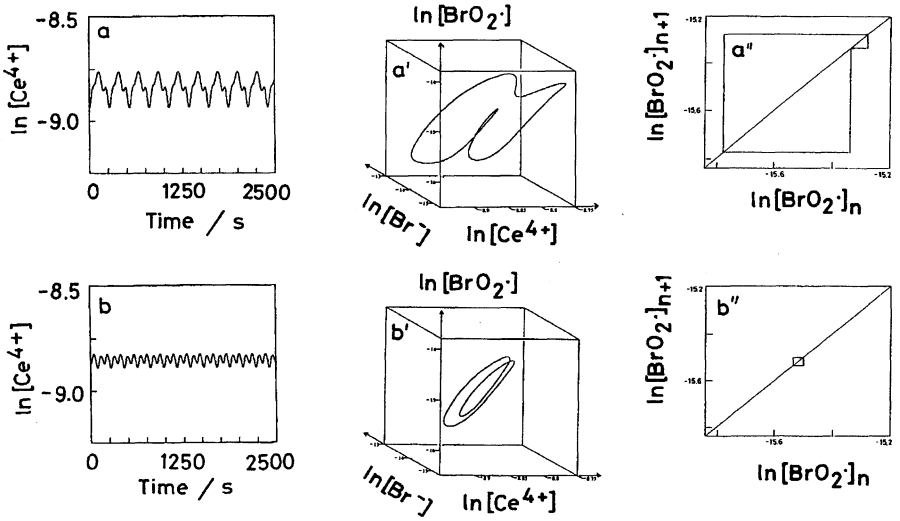

Fig. 7. Coexistence of 1/3 and 1/2 harmonic modes. $\alpha = 0.225$ and $\omega_p = 0.705$ rad s^{-1}. a (oscillation pattern of [Ce^{4+}]), a′ (attractor), and a″ (return map): 1/3 (1/3) harmonic mode. b, b′, and b″: 1/2 (2/2) harmonic modes.

harmonic modes.

Figure 9 shows the dependency of the amplitude of the [Ce^{4+}] oscillations on the magnitudes of the perturbation parameters, α and ω_p, where A_0 represents the amplitude of the natural oscillations. In weakly perturbed cases (α: 0.02 and 0.05), there were maxima in all entrained harmonic modes, whose positions were approximately equal to the corresponding ω_p/ω_0 values. The amplitudes did not increase remarkably at the maxima. The change in the A/A_0 value was indeed large (from 1.67 to 0.85) under the condition that $\alpha = 0.3$. The characteristics of the 1/1 harmonic modes in largely perturbed cases (α: 0.15 and 0.3) were different from those of the others, as shown in this figure.

Simulation at Point B. The entrainment bands calculated at the point are shown in Fig. 10, where the numbers are defined in the same manner as in Fig. 4. The winding numbers constituted the Farey series in weakly perturbed cases. There were no period-doubling bifurcations in front

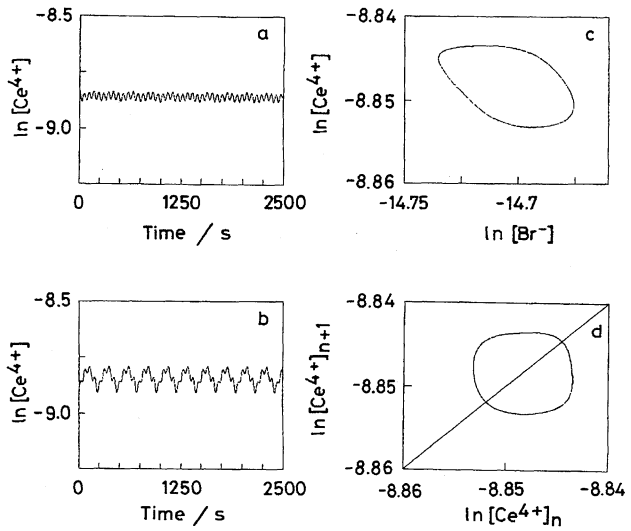

Fig. 8. Coexistence of 1/4 harmonic and quasiperiodic modes. $\alpha = 0.3$ and $\omega_p = 0.1042$ rad s^{-1}. a: quasiperiodic mode, b: 1/4 (1/4) harmonic mode, c and d: Poincaré section ($\cos \omega_p t = 1$) and return map of the quasiperiodic oscillations (a), respectively.

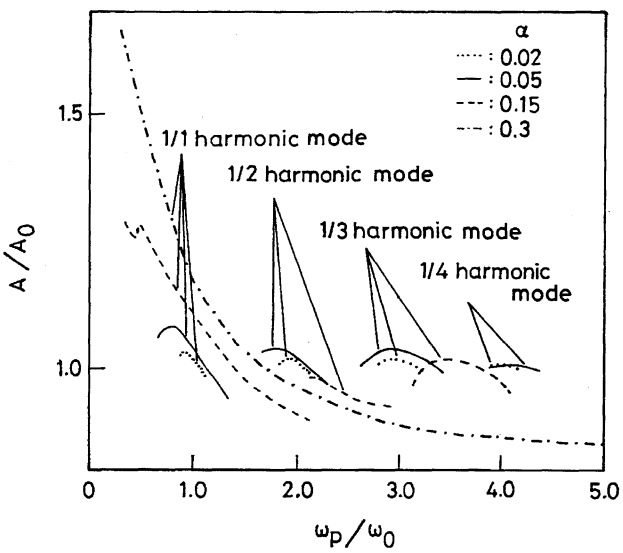

Fig. 9. Dependence of the amplitude of [Ce^{4+}] oscillations on the magnitude of ω_p.
α: dotted curve-0.02, solid curve-0.05, dashed curve-0.15, and alternate dot and dash curve-0.3.

of the left-hand sides of the fundamental 1/1 and 1/2 entrainment bands. Arnol'd tongues were also observed. The system possessed two chaotic regions at this point. One chaotic region appeared between the fundamental 1/2 and 1/3 entrainment regions, and was in contact with a quasiperiodic region (α: 0.095 and 0.12).[30] This chaotic behavior was similar to that at point A. The other chaotic regions appeared between the fundamental 1/1 and 1/2 entrainment regions in the case that $\alpha = 0.04$, and were in contact with no qusiperiodic region.[30] Speaking of the latter chaos, the reaction system at first changed from the 1/1 ($w = 1/1$) harmonic state to a 1/3 (3/3) harmonic state, and fell into a chaotic mode via successive period-doubling bifurcations as the ω_p value increased (Fig. 11a). The system then changed from the

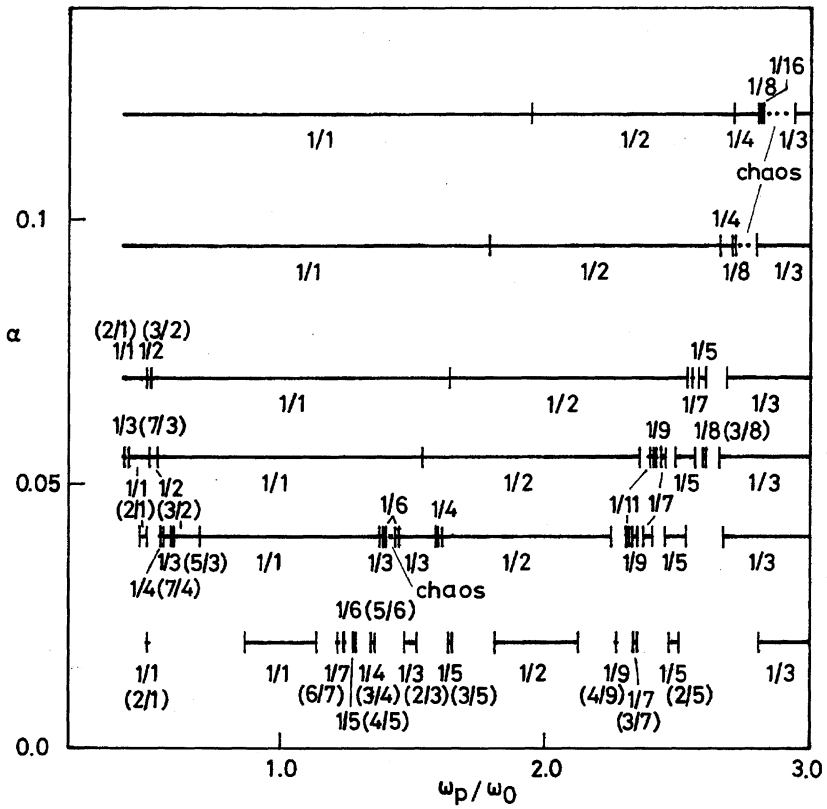

Fig. 10. Entrainment bands (II). The CSTR condition: B. The numbers in the parentheses represent winding numbers.

chaotic mode to a 1/3 (2/3) harmonic mode via reversed period-doubling bifurcations. A 1/1 harmonic entrainment was found at about 0.0346 of the ω_p value in the 1/3 entrainment region (Fig. 11a). This region was a coexisting region of the 1/1 and 1/3 harmonic modes. There was another chaotic region between the 1/3 (2/3) and 1/2 (1/2) entrainment regions. A typical chaotic behavior is also shown in Fig. 11 (α: 0.04 and ω_p: 0.0353 rad s^{-1}). The Fourier spectrum of the [Ce^{4+}] oscillations (Fig. 11c), the Poincaré section (Fig. 11d), and the return map (Fig. 11e) supported the chaotic mode.

The concepts, entrainment, Farey series, quasiperiodic oscillations, and chaos, have been produced in studies of many mathematical models. In some experimental studies, entrainment, Farey series, and quasiperiodicity were recognized.[12,13,16–20] We sketched a global profile of the forced minimal oscillator in this study as well as two types of chaos, and the coexistence of two oscillation modes were newly simulated. The existence of small-amplitude oscillations was estimated by Taylor and Geiseler and confirmed experimentally.[14] It was estimated here again. However, the simulation of chaos was quite different from their's. Chaos was observed in forced nervous systems.[19,20] However, there has been no report concerning homogeneous forced-chemical systems.[31] The wave patterns of [Ce^{4+}] oscillations in this study (particularly the presence of notches in Figs. 7a and 8b) were similar to those observed in the forced minimal oscillator experimentally.[15] We often encountered slowing-down effects when an oscillatory mode changed (for example in an entrainment edge or in regions of successive period-doubling bifurcations). When a slowing down occurred, many transient times (3×10^5 s at maximum) were needed (usually less than 3×10^3 s). Buchholz et al. observed a slow change at the entrainment edges in a forced BZ reaction (slow change in the Fourier spectrum with time).[12] While the critical slowing down in this study is similar to the slow change in the experiment, we do not know at present whether both slowing-down activities are the same or not. The difference in the entrainment bands of points A and B was not obvious in this study.

There are still some doubts concerning this study: Why does entrainment (chaos and small-amplitude oscillations, etc.) occur? We cannot resolve the problems, because the differential equations derived from the FKN mechanism are too complicated to be mapped. If we allow the presence of chaos (namely an interval map), we can compare the results (the existence of small-amplitude oscillations and the coexistence of two harmonic modes) with the behaviors of one-dimensional dynamical systems.[28] Here, we wish to focus on entrainment in a weakly perturbed case and discuss a kicked oscillator reported by Ding, which seemed to be a prototype

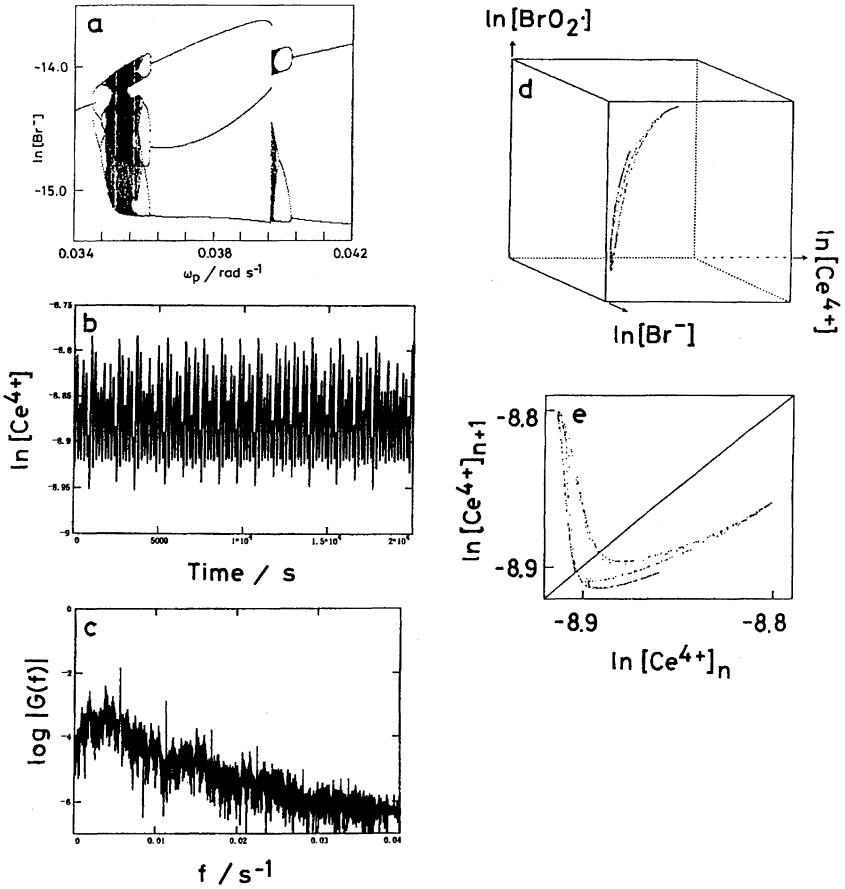

Fig. 11. Chaotic mode (II) $\alpha = 0.04$ and $\omega_p = 0.0353$ rad s^{-1}. a: bifurcation diagram between fundamental 1/1 and fundamental 1/2 entrainment bands, depending on the magnitude of ω_p. b, c, d, and e: oscillation pattern of [Ce^{4+}], its Fourier spectrum, Poincaré section ($\cos \omega_p t = 1$), and return map, respectively.

of forced oscillators.[32] The concept "phase-shifting" obtained during this study is the same as "phase-resetting" mentioned by Hoppensteadt and Keener.[33]

We define a stable limit cycle as

$$dr/dt = sr(1-r^2),\ d\theta/dt = 1. \tag{9}$$

It is assumed that the oscillator is subjected to a periodic force (period: T_p) in the x direction. The representative point takes off the limit cycle ($r = 1$) for perturbations and relaxes to the limit cycle. The parameter s is a measure of the inverse of the relaxation time. The behavior of this system is represented by the following differential equations:

$$\begin{aligned} dx/dt &= sx(1-x^2-y^2) - y + 2\varkappa\Sigma\delta(t-2\pi n\beta), \\ dy/dt &= x + sy(1-x^2-y^2), \end{aligned} \tag{10}$$

where

$$\beta = T_p/2\pi \quad (= 1/\omega_p). \tag{11}$$

The summation is over all integers (n). We now assume that the system rapidly relaxes to the limit cycle after a kick ($s \to \infty$). As shown in Fig. 12a, r_n and θ_n after the nth "kick" change into $r_n{}^*$ ($= 1$) and $\theta_n{}^*$ ($= \theta_n + 2\pi\beta$) before the (n+1) th "kick". Thus, r_{n+1} and θ_{n+1} are related to r_n and θ_n as follows:

$$\begin{aligned} r_{n+1} &= \{[2\varkappa + \cos(\theta_n + 2\pi\beta)]^2 + \sin^2(\theta_n + 2\pi\beta)\}^{1/2}, \\ \tan\theta_{n+1} &= \sin(\theta_n + 2\pi\beta)/[2\varkappa + \cos(\theta_n + 2\pi\beta)]. \end{aligned} \tag{12}$$

Equation 12 is a one-dimensional circle map with two parameters. $\varkappa$ is a measure of the amplitude of the external perturbation and β the ratio of two frequencies. When $\varkappa > 1/2$ (strongly perturbed case), the map does not possess a quasiperiodic mode. Therefore, this discussion is restricted to a weak perturbation ($\varkappa \leqq 1/2$). Figure 12b shows entrainment bands of the kicked oscillator in the β–$\varkappa$ plane, which

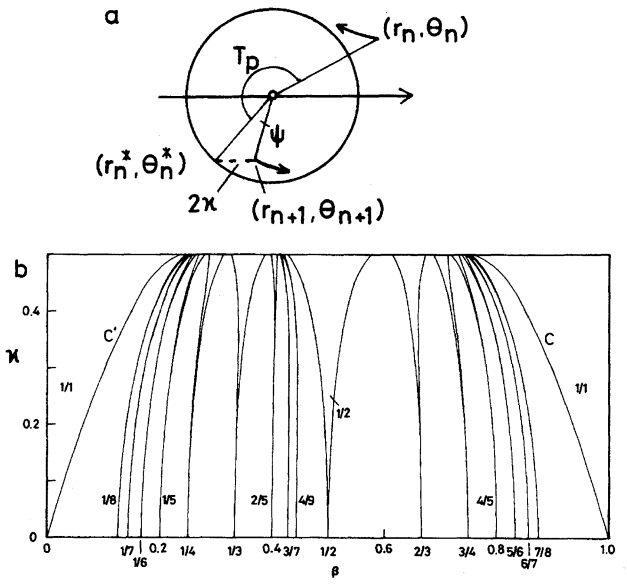

Fig. 12. Profile of kicked oscillator. a: the kicked oscillator and phase-shift, b: entrainment bands of the kicked oscillator stimulated by a weak perturbation.

was obtained from bifurcation diagrams calculated by Eq. 12. The Farey series and Arnol'd tongues were simulated in this figure. We discuss the simplest 1/1 entrainment and formulate curve c in Fig. 12b. When the system is kicked at the point ($r_n{}^*$, $\theta_n{}^*$), the phase of the system increases by ψ in the case that $\theta_n{}^* > \pi$. Because we assume rapid relaxation, a kick having a period of $2\pi-\psi$ corresponds to the 1/1 entrainment. ψ is written as

$$\cos\psi = (1 + 2\varkappa\cos\theta_n{}^*)/\sqrt{1 + 4\varkappa^2 + 4\varkappa\cos\theta_n{}^*}. \tag{13}$$

When $\cos\theta_n{}^* = -2\varkappa$, the maximum of ψ is obtained,

$$\cos\psi_{max} = \sqrt{1-4\varkappa^2}. \tag{14}$$

Therefore, curve c is represented as

$$\beta_{min} = 1 - (1/2\pi)\arccos\sqrt{1-4\varkappa^2}. \tag{15}$$

Equation 15 reproduces curve c in Fig. 12b well. If $\theta_n{}^* < \pi$, we can obtain curve c'. Thus, the 1/1 entrainment of a kicked oscillator was interpreted by the phase-shifting term. While the formulation of other entrainments was difficult, the entrainments may be qualitatively interpreted using the same term. Marek studied the behaviors of a forced BZ rection in CSTR (with spikes of solutions of Br^- or Ce^{4+}), and reported phase-shifting in the oscillations of ln ($[Ce^{4+}]/[Ce^{3+}]$).[34] In a forced minimal oscillator, even a qualitative interpretation of entrainment is difficult. We wish that the discussion concerning a kicked oscillator may be useful in understanding the entrainment of a forced minimal oscillator.

References

1 M. Fugimoto, "Kanwagensho no Kagaku," ed by K. Azuma and S. Nagakura, Iwanami Shoten, Tokyo (1973), p. 313.

2 T. Yasunaga and M. Harada, "Shin Jikken Kagaku Koza," ed by Nippon Kagaku Kai, Maruzen, Tokyo (1978), Vol. 16, p. 386.

3 H. Shimizu, p. 5 in Ref. 1.

4 "Oscillations and Traveling Waves in Chemical Systems," ed by R. J. Field and M. Burger, Wiley-Interscience, New York (1985).

5 W. C. Troy, p. 145 in Ref. 4.

6 Y. Sasaki, *Bull. Chem. Soc. Jpn.*, **63**, 1700 (1990).

7 F. W. Schneider, *Annu. Rev. Phys. Chem.*, **36**, 347 (1985).

8 P. Rehmus and J. Ross, p. 287 in Ref. 4.

9 "Temporal Order," ed by L. Rensing and N. I. Jaeger, Springer-Verlag, Berlin, Heidelberg, New York, and Tokyo (1985).

10 T. Kai and K. Tomita, *Prog. Theor. Phys.*, **61**, 54 (1979).

11 T.-M. Kruel, A. Freund, and F. W. Schneider, *J. Chem. Phys.*, **93**, 416 (1990).

12 F. Buchholz, A. Freund, and F. W. Schneider, p. 116 in Ref. 9.

13 M. Dolník, J. Finkeová, I. Schreiber, and M. Marek, *J. Phys. Chem.*, **93**, 2764 (1989).

14 T. W. Taylor and W. Geiseler, *Ber. Bunsenges. Phys. Chem.*, **89**, 441 (1985).

15 W. Hohmann, D. Lebender, J. Müller, N. Schinor, and F. W. Schneider, *J. Phys. Chem.*, **101**, 9132 (1997).

16 A. Karantonis, M. Pagitsas, and D. Sazou, *Chaos*, **3**, 243 (1993).

17 Y. Osada, K. Umezawa, and A. Yamauchi, *Bull. Chem. Soc. Jpn.*, **62**, 3232 (1989).

18 G. Matsumoto, K. Kim, K. Uehara, and J. Shimada, *J. Phys. Soc. Jpn.*, **49**, 906 (1980).

19 K. Aihara, G. Matsumoto, and Y. Ikegami, *J. Theor. Biol.*, **109**, 249 (1984).

20 K. Aihara, T. Numajiri, G. Matsumoto, and M. Kotani, *Phys. Lett. A*, **116**, 313 (1986).

21 R. J. Field, E. Körös, and R. M. Noyes, *J. Am. Chem. Soc.*, **94**, 8649 (1972).

22 W. Geiseler and K. Bar-Eli, *J. Phys. Chem.*, **85**, 908 (1981).

23 K. Bar-Eli and W. Geiseler, *J. Phys. Chem.*, **87**, 3769 (1983).

24 Y. Sasaki, *Bull. Chem. Soc. Jpn.*, **61**, 4071 (1988).

25 R. J. Field and H.-D. Försterling, *J. Phys. Chem.*, **90**, 5400 (1986).

26 C. W. Gear, "Numerical Initial Value Problems in Ordinary Differential Equations," Prentice-Hall, Englewood Cliffs, N. J. (1971), Chap. 11.

27 When we count m in the entrained oscillations of $[Ce^{4+}]$, notches (small peaks and shoulders which generate "directly" from the periodic perturbation) should be neglected. For example the m values in Figs. 7a and 8b are equal to 1.

28 Y. Sasaki, submitting in this Bulletin.

29 M. H. Jensen, P. Bak, and T. Bohr, *Phys. Rev. Lett.*, **50**, 1637 (1983).

30 The chaos and coexistence of two oscillation modes in this system is discussed in Ref. 28.

31 Chaos has been reported in the non-forced BZ reaction. See a review by: I. R. Epstein and K. Showalter, *J. Phys. Chem.*, **100**, 13132 (1996), and references cited therein.

32 E. J. Ding, *Phys. Rev. A*, **35**, 2669 (1987).

33 F. C. Hoppensteadt and J. P. Keener, *J. Math. Biol.*, **15**, 339 (1982).

34 M. Marek, p. 105 in Ref. 9.